Further Investigation of the Effect of Elongational Viscosity on Entrance Flow

DEBABRATA SARKAR AND MAHESH GUPTA*
Mechanical Engineering-Engineering Mechanics Department
Michigan Technological University
Houghton, MI 49931

ABSTRACT: A new model for strain-rate dependence of elongational viscosity of a polymer is introduced. The proposed model can capture the initial strain thickening, which is followed by a descent in elongational viscosity as the elongation rate is further increased. Effect of the four rheological parameters in the new model on a 4:1 entrance flow is analyzed. It is confirmed that the entrance pressure loss and recirculating vortices in an entrance flow grow significantly as the Trouton ratio is increased. The center-line velocity near the abrupt contraction in a 4:1 entrance flow is found to overshoot its value for a fully developed flow in the downstream channel, if the Trouton ratio has a local minima beyond the Newtonian limit of the polymer.

INTRODUCTION

IN CONTRAST TO low molecular weight fluids, the shear and elongational viscosities of a polymer depend upon strain rate. The strain-rate dependence of the shear viscosity of various polymers has been extensively reported in the literature [1]. At low values of strain rate, the shear viscosity of a polymer is constant, whereas at higher strain rates beyond the Newtonian limit, the shear viscosity decreases with strain rates. Various empirical equations, such as Carreau-Yasuda model [2,3] and Cross model [4], can accurately capture the Newtonian as well as the shear-thinning behavior of the polymer viscosity. The strain-rate dependence of the elongational viscosity of polymers is not as well established. At low elongation rates (Newtonian limit), the experimental data in the literature [1,5] show that the elongational viscosity of polymers is constant and the Trouton ratio (Tr), which is defined as the ratio of elongational viscosity to shear viscosity, is the same as that for Newtonian fluids. That is, $Tr = 3$ for an axisymmetric flow, whereas $Tr = 4$ for a planar flow. Due to the inherently unsteady nature of elongational flows, direct

*Author to whom correspondence should be addressed.

0731-6844/01/17 1473–12 $10.00/0 DOI: 10.1106/TTQL-9UB4-4EBW-AAX3

measurement of elongational viscosity at high elongation rates is difficult. The limited experimental data available in the literature shows different trends for different polymers. Beyond the Newtonian limit, the elongational viscosity of a polymer may decrease (e.g., HDPE [6]), remain constant (e.g., Polyisobutylene-isoperene copolymer [7], PS [5]), may initially increase followed by a descent (e.g., LDPE [8]). Therefore, beyond the Newtonian limit, Trouton ratio for polymers depends upon strain rate.

Since the Trouton ratio for generalized Newtonian fluids [1] is independent of strain rate, an elongation-dominated flow simulated by using such a formulation often has a large discrepancy with the actual polymeric flow. A strain-rate-dependent Trouton ratio can be obtained by adjusting various material parameters in a viscoelastic model [9]. However, to accurately capture the elongational viscosity of a polymer, a large number of material parameters are generally required in a viscoelastic constitutive equation. Uncertainty of the convergence of a viscoelastic formulation makes it even less attractive for simulation of complex polymeric flows [10–18].

To circumvent the complexities of a viscoelastic flow simulation, several authors have attempted to develop a composite viscosity model combining the shear and elongational viscosities in the generalized Newtonian formulation. Since the third invariant of the strain-rate tensor ($\tilde{e}(\nabla\hat{\mathbf{v}} + \nabla\hat{\mathbf{v}}^T)/2$) is zero for a simple shear, but is (3/4 × elongation rate) for an axisymmetric elongation, equations depending upon the second (e_{II}), and third (e_{III}) invariants of the strain rate tensor have been used for such a composite viscosity model [19–21]. However, this approach cannot be extended to a planar extension or three-dimensional extension because in a planar extension $e_{III} = 0$. To include the effect of elongational viscosity in a mold filling simulation, Moller et al. [19] used an equation for viscosity which depends upon an eigenvalue of the strain-rate tensor in the plane of a thin shell finite element. Again, this approach cannot be extended to a three-dimensional flow.

To develop a viscosity model which can be used for a planar as well as axisymmetric flow, Schunk and Scriven [22] employed a weighted average of the shear and elongational viscosities. In this model the shear and elongational viscosities depend only upon e_{II}, but the weighting function depends upon a magnitude of vorticity tensor which is independent of the solid body rotation. Similar approach was reported by Souza Mendes et al. [23,24], who used a geometric mean instead of arithmetic mean of shear and elongational viscosities.

To include the effects of elongational viscosity (η_e) and the first normal stress difference (N_1) on the polymeric flow in planar channels, Mitsoulis et al. [25] used the following fluid model:

$$\tau_{xx} = \eta_0 e_{xx} + \Psi_1 e_{xy}^2, \qquad \tau_{yy} = \eta_0 e_{yy}, \qquad \tau_{xy} = \eta_s e_{xy} \tag{1}$$

where $\underline{\underline{\tau}}$ and $\underline{\underline{e}}$ are components of the stress and strain-rate tensors respectively, η_s and Ψ_1 are, respectively, the strain-rate-dependent shear viscosity and first normal stress difference, and η_0 is the zero-shear-rate viscosity. In Equations (1)–(3), the x direction is along the axis of the channel with y being perpendicular to the axis. Since this approach suggested by Mitsoulis et al. is not frame invariant, it has only a limited applicability.

More recently, Gupta [26–29] presented a frame invariant simulation of a 4:1 entrance flow using independent shear and elongational viscosities. The shear and elongational viscosities in this approach are functions of e_{II} only and simulation can be extended to a planar [29] as well as a three-dimensional flow [27]. To analyze the effect of elongational viscosity on the flow in a channel with an abrupt contraction, Gupta [26–29] used the truncated power-law model for the shear as well as elongational viscosity. In this paper a new model for strain-rate-dependence of elongational viscosity is introduced. The new model can capture the various trends in elongational viscosities for different polymers mentioned earlier in this paper.

ELONGATIONAL VISCOSITY MODEL

For the shear viscosity of a polymer, the Carreau model [2] has been used in this paper:

$$\eta_s = \eta_0[1+(\lambda e_{II})^2]^{(n-1)/2} \tag{2}$$

where η_0 is the zero-shear-rate viscosity, λ characterizes the strain rate for transition between Newtonian and power-law regions, n is the power-law index and $e_{II} = \sqrt{2\tilde{e} : \tilde{e}}$. Following the approach used by Gupta [26–29], in this paper the elongational viscosity has also been represented as a function of e_{II}. For polymers such as polystyrene [5] and HDPE [6], which have a constant or strain-thinning elongational viscosity, the variation of elongational viscosity with e_{II} can be represented by an equation such as the Carreau model [Equation (2)]. To capture the behavior of elongational viscosity of polymers such as LDPE [8], which exhibit an increase in elongational viscosity beyond the Newtonian range, followed by a power-law-type descent as the strain rate is further increased, we propose the following model for elongational viscosity of a polymer:

$$\eta_e = \eta_0\left[3+\delta\left\{1-\frac{1}{\sqrt{1+(\lambda_1 e_{II})^2}}\right\}\right][1+(\lambda_2 e_{II})^2]^{(m-1)/2} \tag{3}$$

It is noted that the elongational viscosity model in Equation (3) is an enhancement of the Carreau model [Equation (2)]. Based upon the experimental observations reported in the literature [1,5], at low strain rates the elongational

viscosity of $3\eta_0$, where η_0 is the Newtonian limit of shear viscosity, has been enforced in Equation (3). As shown in Figure 1, the parameter λ_1 in Equation (3) specifies $1/e_{II}$ for the transition between Newtonian and elongation-thickening portions of the viscosity strain-rate curve, whereas δ characterizes the total increase in viscosity in the elongation-thickening portion. Parameters λ_2 and m in Equation (3) specify $1/e_{II}$ for transition between elongation-thickening and power-law region, and the power-law index for elongational viscosity, respectively. It should be noted that for $\delta = 0$, $\lambda_2 = \lambda$ and $m = n$, the elongational viscosity obtained by using Equation (3) is the same as the elongational viscosity predicted by a generalized Newtonian formulation with Carreau model for shear viscosity, that is, $\eta_e = 3\eta_s$.

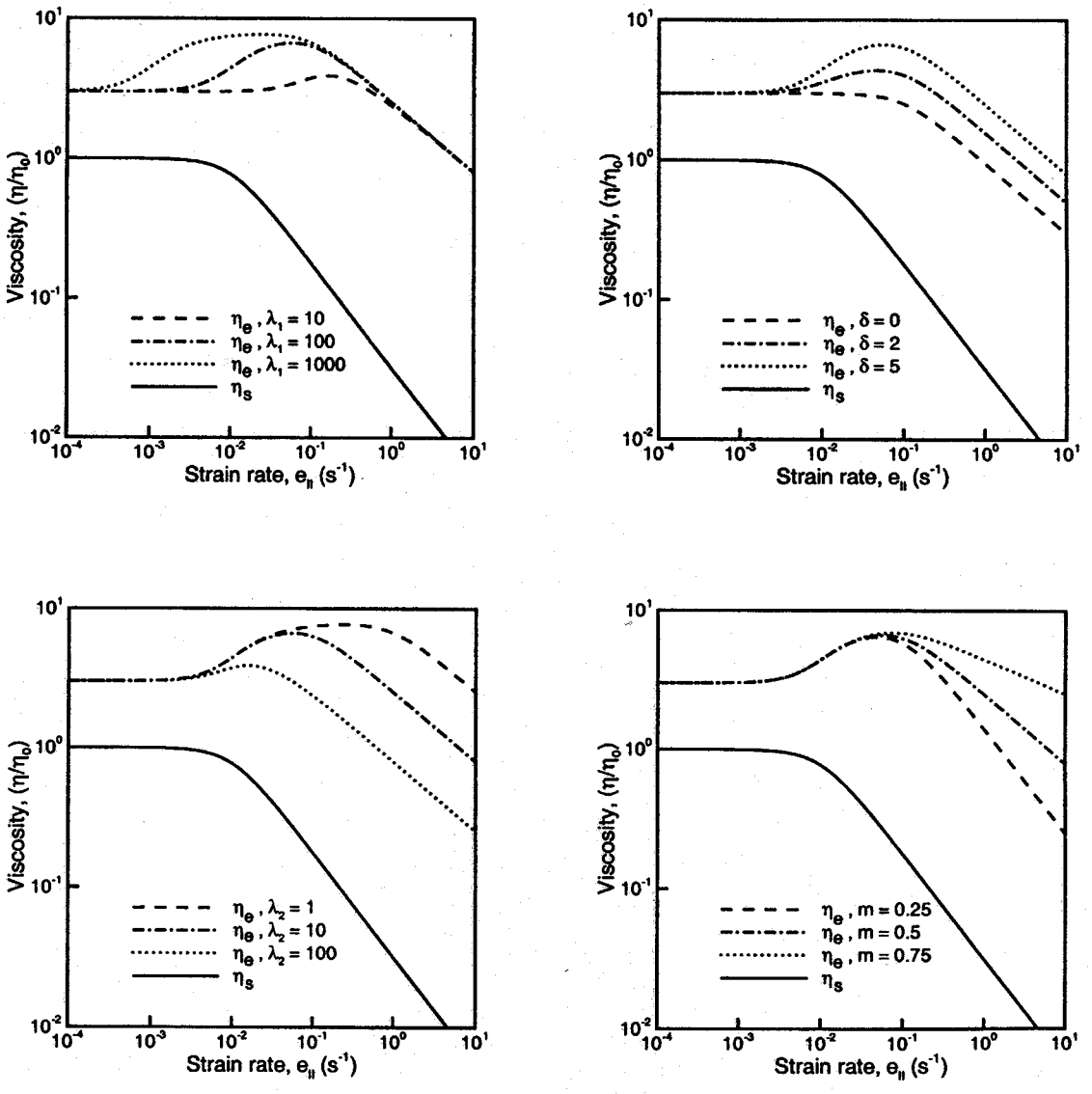

Figure 1. *Effect of various parameters in Equation (3) on elongational viscosity. For all four plots, the values of the elongational viscosity parameters which remain constant are:* $\delta = 5$, $\lambda_1 = 100$, $\lambda_2 = 10$, *and* $m = 0.5$.

EFFECT OF ELONGATIONAL VISCOSITY PARAMETERS ON ENTRANCE FLOW

Since the flow near an abrupt contraction in a channel (entrance flow) is highly elongation dominated, it has been extensively used in the literature to analyze the effect of elongational viscosity on polymeric flows [7,26–29]. To maintain the elongational flow near the abrupt contraction, if the elongational viscosity of the fluid is high, a large pressure gradient is required near the abrupt contraction. The extra pressure drop near the abrupt contraction, called entrance loss, is typically expressed in terms of an equivalent length of the downstream channel:

$$L_e = \frac{\Delta p - \Delta p_1 - \Delta p_2}{\partial p_2} \tag{4}$$

where Δp denotes the total pressure drop in the channel, Δp_1 and Δp_2 are, respectively, the pressure drop for fully developed flow in the portions of the channel upstream and downstream of the abrupt contraction and ∂p_2 is the magnitude of the pressure gradient for fully developed flow in the downstream channel.

For a constant flow rate in the channel, as expected, the velocity along the center line of the channel increases sharply near the abrupt contraction. Keeping the shear viscosity the same, if the elongational viscosity of a fluid is increased, fluid has a lesser tendency to elongate. Consequently, such an increase in elongational viscosity results in a larger distance for the center-line velocity to reach its value for a fully developed flow in the downstream channel and a smaller value of the center-line velocity at the location of the abrupt contraction [28]. In contrast, near the abrupt contraction, the experimental data in literature on entrance flow [30], sometimes shows an overshoot in the center-line velocity in comparison to its value for a fully developed flow in the downstream channel. It is shown later in this paper that such an overshoot in the center-line velocity is observed if for a range of strain rate, the Trouton ratio decreases as the strain rate is increased.

Using the truncated power-law model for shear as well as elongational viscosity, effects of the elongational power-law index (m), strain rate for the onset of power-law region ($1/\lambda_2$) and the flow rate on the velocity and pressure distributions in a 4:1 entrance flow was analyzed by Gupta [28]. Gupta found that for a fixed shear viscosity, as the Trouton ratio is increased by increasing m, $1/\lambda_2$ or flow rate, the entrance loss and recirculating vortices near the abrupt contraction grow significantly and a larger distance is required for the center-line velocity to develop in the downstream channel. Similar effects of m, λ_2 and flow rate are observed if instead of the truncated power-law model, the Carreau model is used for the shear and elongational viscosities. The effect of the strain rate for the onset of the elongational thickening region ($1/\lambda_1$) and total increase in the viscosity in the elongational thickening region (δ), which could not be analyzed with the truncated power-law model for the two viscosities, is analyzed next in this paper. Also,

Gupta [28] analyzed the effect of λ_2 on entrance flow for $\lambda_2 < \lambda$. Effect of λ_2 on entrance flow for $\lambda_2 > \lambda$ is also analyzed later in this paper. Length of the upstream and downstream channels in the finite element mesh used are $20r$ and $30r$, respectively, where r is the radius of the downstream channel. For all the entrance flow simulations reported in this paper, the Carreau model parameters for the shear viscosity are $\lambda = 10$ s and $n = 0.25$, and the results have been normalized with respect to η_0.

Effect of δ

An increase in δ increases the Trouton ratio in the strain-thickening portion of the elongational viscosity. Even though the strain rate for the onset of elongation-thinning region and slope of the elongational viscosity curve in the power-law region remain unchanged if λ_2 and m are fixed, the elongational viscosity line in the power-law region moves upward as δ is increased. Therefore an increase in δ also increases the Trouton ratio in the power-law region. With the flow rate and all other elongational viscosity parameters fixed ($\dot{\gamma}_a = 1\ s^{-1}$, $\lambda_1 = 10$ s, $\lambda_2 = 0.1$ s, $m = 0.5$), the effect of δ on the recirculating vortices in a 4:1 entrance flow is shown in Figure 2. Since the power-law index for elongational viscosity is larger than that for the shear viscosity ($n = 0.25$), even for $\delta = 0$, the Trouton ratio increases with strain rate. Therefore, a significantly large recirculating vortex is observed for $\delta = 0$ in Figure 2. Since the flow rate for the flow distributions shown in Figure 2 is in the elongation-thickening region of the elongational viscosity, the Trouton ratio for the velocity distributions shown in Figure 2 increases as δ is increased. Therefore, the recirculating vortex near the abrupt contraction in Figure 2 grows significantly as δ is increased.

For the three values of δ, Figure 3 shows the velocity and pressure along the axis of the 4:1 entrance flow. In Figure 3, $z = 0$ corresponds to the location of abrupt contraction. Since the Trouton ratio increases as δ is increased, a larger distance is required for the center-line velocity to reach its fully developed value. It is also noted that the center-line velocity in a 4:1 entrance flow simulation using the truncated power-law model has a sharp kink at the location of abrupt contraction [28], whereas the center-line velocity in Figure 3 using Carreau model and Equation (3) for elongational viscosity has a smooth variation near the abrupt contraction. The kink in the center-line velocity reported in [28] is probably due to an abrupt change in slope of the viscosities at the Newtonian limit of the truncated power-law model. The entrance pressure loss, which corresponds to the sharp drop in pressure near the abrupt contraction in Figure 3, increases significantly as δ, and hence the Trouton ratio is increased.

Effect of λ_1

For $\delta > 0$, an increase in λ_1 reduces the strain rate for the onset of strain-thicken-

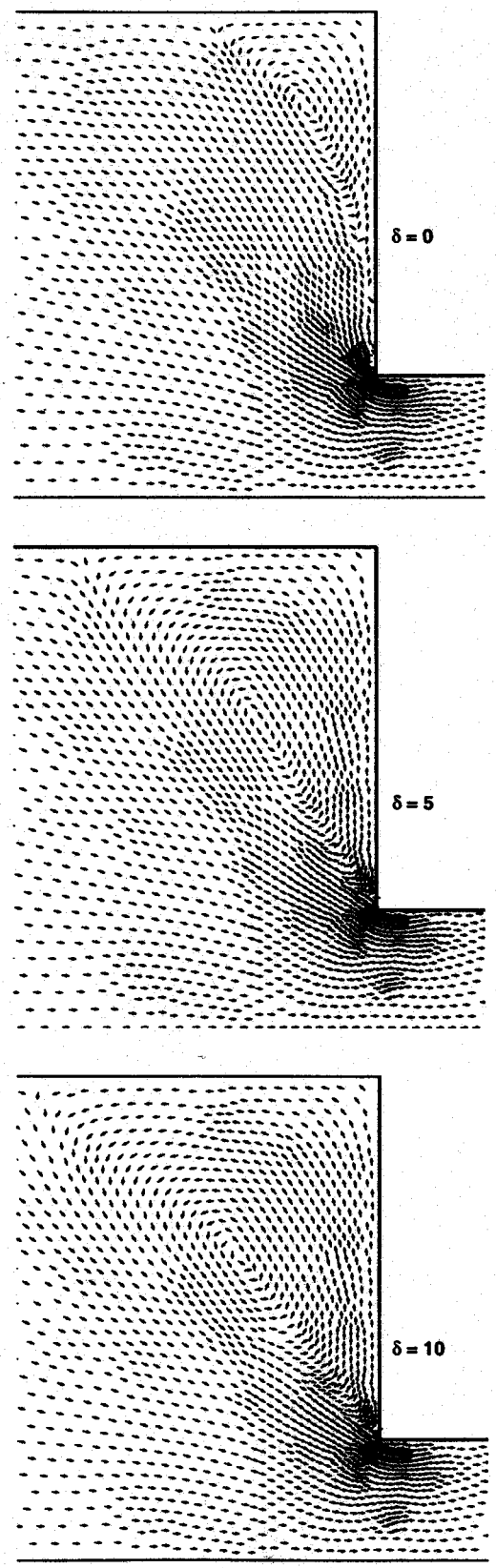

Figure 2. *Effect of on the recirculation in a 4:1 abrupt contraction for* $\lambda = 10$, $n = 0.25$, $\lambda_1 = 10$ *s*, $\lambda_2 = 0.1$ *s*; $m = 0.5$ *and* $\dot{\gamma}_a = 1\ s^{-1}$.

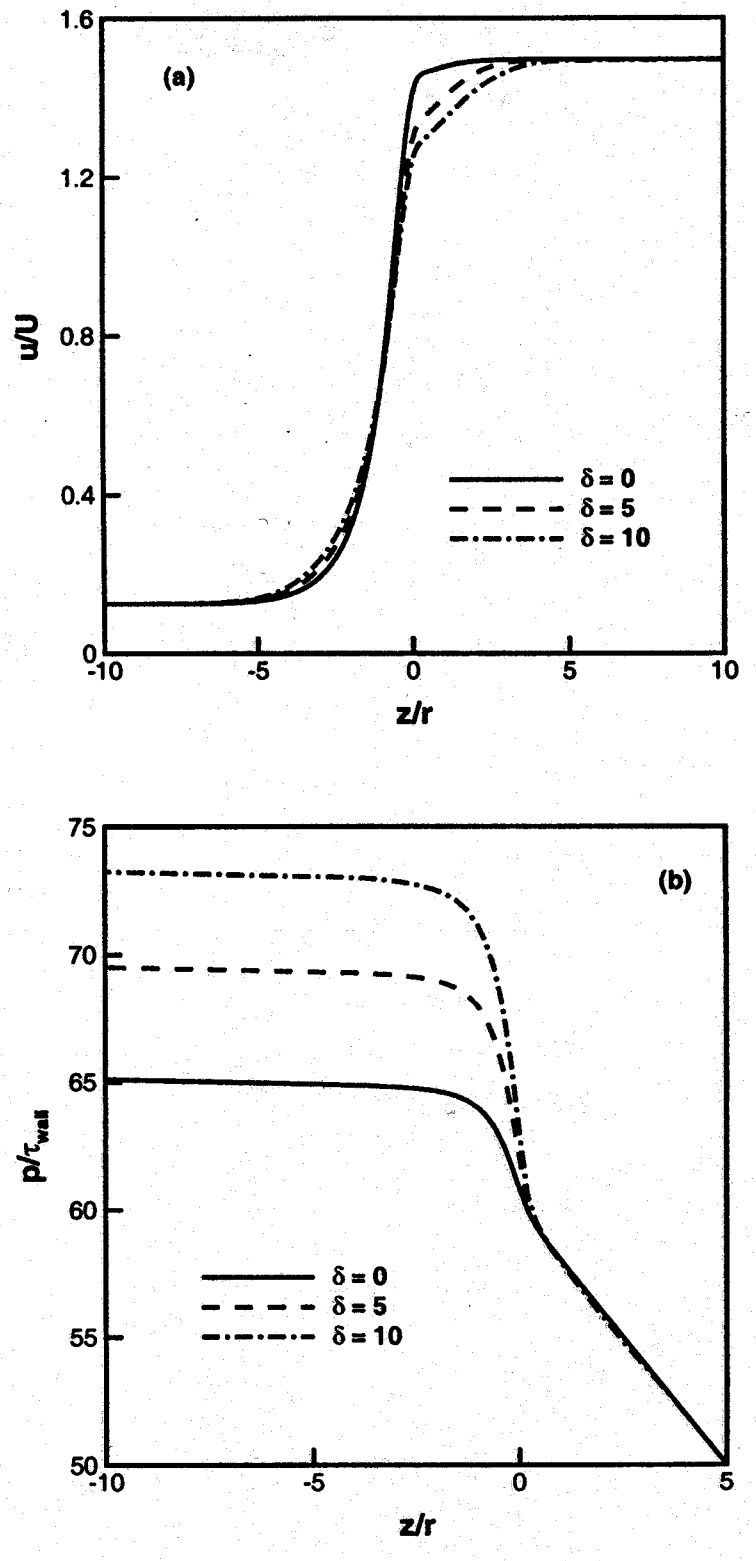

Figure 3. *Effect of δ on the velocity (a) and pressure (b) along the center-line at* $\dot{\gamma}_a = 1\ s^{-1}$ *for* $\lambda = 10$ *s,* $n = 0.25$, $\lambda_1 = 10$ *s,* $\lambda_2 = 0.1$ *s and* $m = 0.5$.

ing region of the elongational viscosity. Therefore, the Trouton ratio in the range of strain rate where the elongational viscosity is in the strain-thickening region for one viscosity curve, and in the Newtonian region for the other curve, the Trouton ratio is higher for the curve with higher λ_1. Beyond this region, λ_1 has little effect on Trouton ratio. For two different values of λ_1 (10 and 100 s), with all the other viscosity parameters being the same ($\delta = 10$, $\lambda_2 = 10$ s, $m = 0.5$), and the flow rate being such that strain rate in the 4:1 entrance flow is in the region where the Trouton ratio is different for two cases ($\dot{\gamma}_a = 0.01\ s^{-1}$), Figure 4 shows the velocity and pressure along the axis of symmetry of the 4:1 entrance flow. For the case with a larger Trouton ratio ($\lambda_1 = 100$ s) in Figure 4, a larger distance is required for the center-line velocity to reach its fully developed value and the entrance loss is larger. It was also confirmed that the recirculating vortex is bigger for $\lambda_1 = 100$ s. It should be noted that for most polymer processing applications the strain rate is expected to be in the power-law region, therefore λ_1 will have only a limited effect on the flow; however, an accurate value of δ is important because δ affects the elongational viscosity in the elongation-thickening as well as in the power-law region.

Effect of λ_2

Effect of λ_2 on entrance flow was analyzed by Gupta [28]. It should be noted that for the truncated power-law model the Newtonian limit for the elongational viscosity is equivalent to $1/\lambda_2$ in Equation (2). Since the Trouton ratio in the power-law region of elongational viscosity increases as λ_2 is decreased, the entrace loss and recirculating vortex grow significantly with a reduction in λ_2 and a larger distance is required for the center-line velocity to develop completely [28]. For all the cases analyzed by Gupta [28], λ_2 is smaller than λ. For $\lambda_2 < \lambda$, the center-line velocity in the 4:1 entrance flow is always smaller than its value for a fully developed flow in the downstream channel. If λ_2 is greater than λ, then for e_{II} between $1/\lambda_2$ and $1/\lambda$, the Trouton ratio decreases as the strain rate is increased. If the Trouton ratio decreases as the strain rate is increased, the fluid along the axis of the channel, which observes a pure elongation deformation, has a greater tendency to elongate. Therefore, in Figure 5(a), for $\lambda_2 > \lambda$, the center-line velocity near the abrupt contraction increases beyond its value for a fully developed flow in the downstream channel. Since the local drop in the Trouton ratio increases as λ_2 is increased, the overshoot in the center-line velocity also increases with λ_2. It should be noted that the first normal stress difference in a polymeric flow, which has not been accounted for in the present work, may also affect the centerline velocity in the vicinity of the abrupt construction. Finally, since the Trouton ratio decreases as λ_2 is increased, in Figure 5(b), the sharp drop in the pressure near the abrupt contraction, that is, entrance loss, decreases as λ_2 is increased.

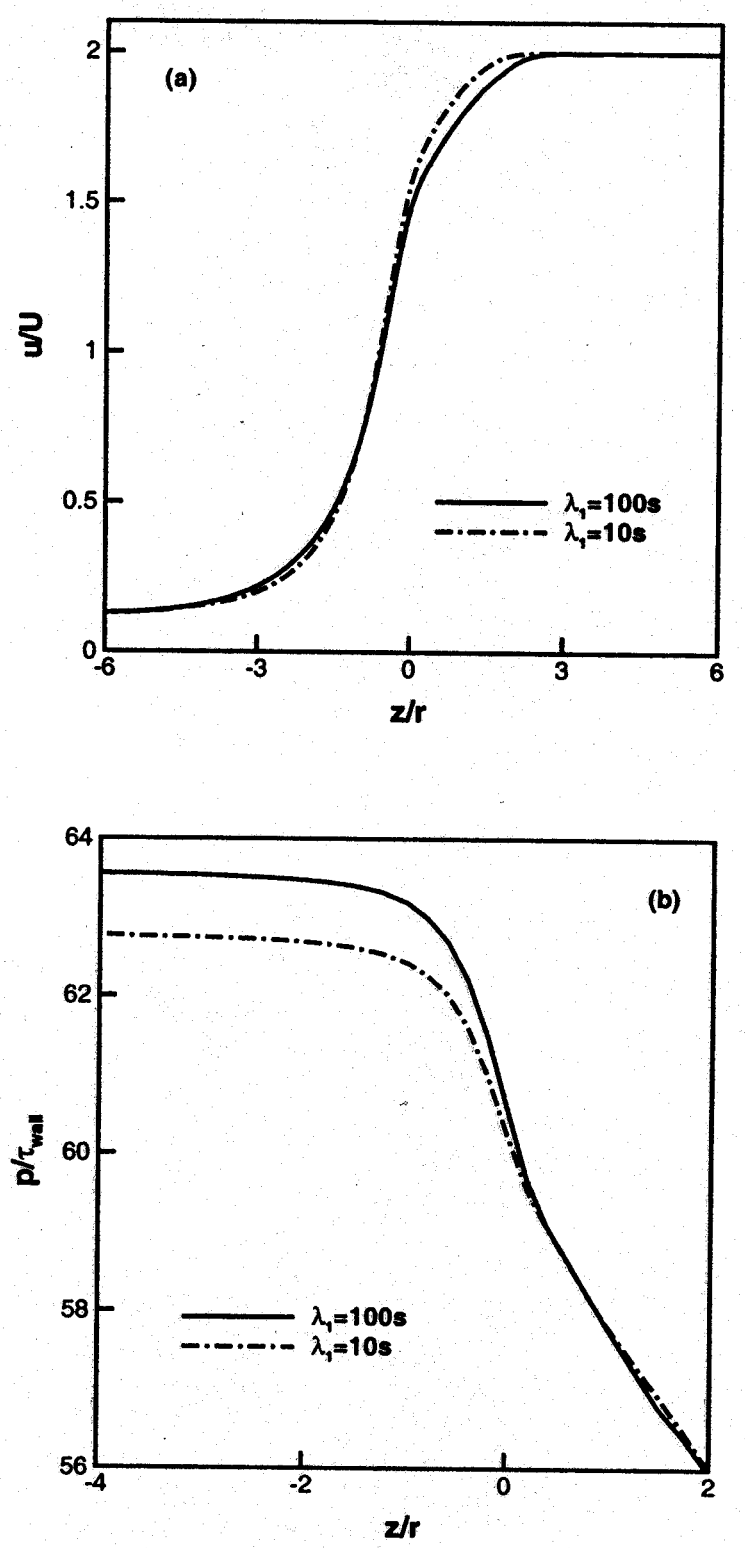

Figure 4. *Effect of λ_1 on the velocity (a) and pressure (b) along the center-line at $\dot{\gamma}_a = 0.01\ s^{-1}$ for $\lambda = 10$ s, n = 0.25, $\delta = 10$, $\lambda_2 = 10$ s and m = 0.5.*

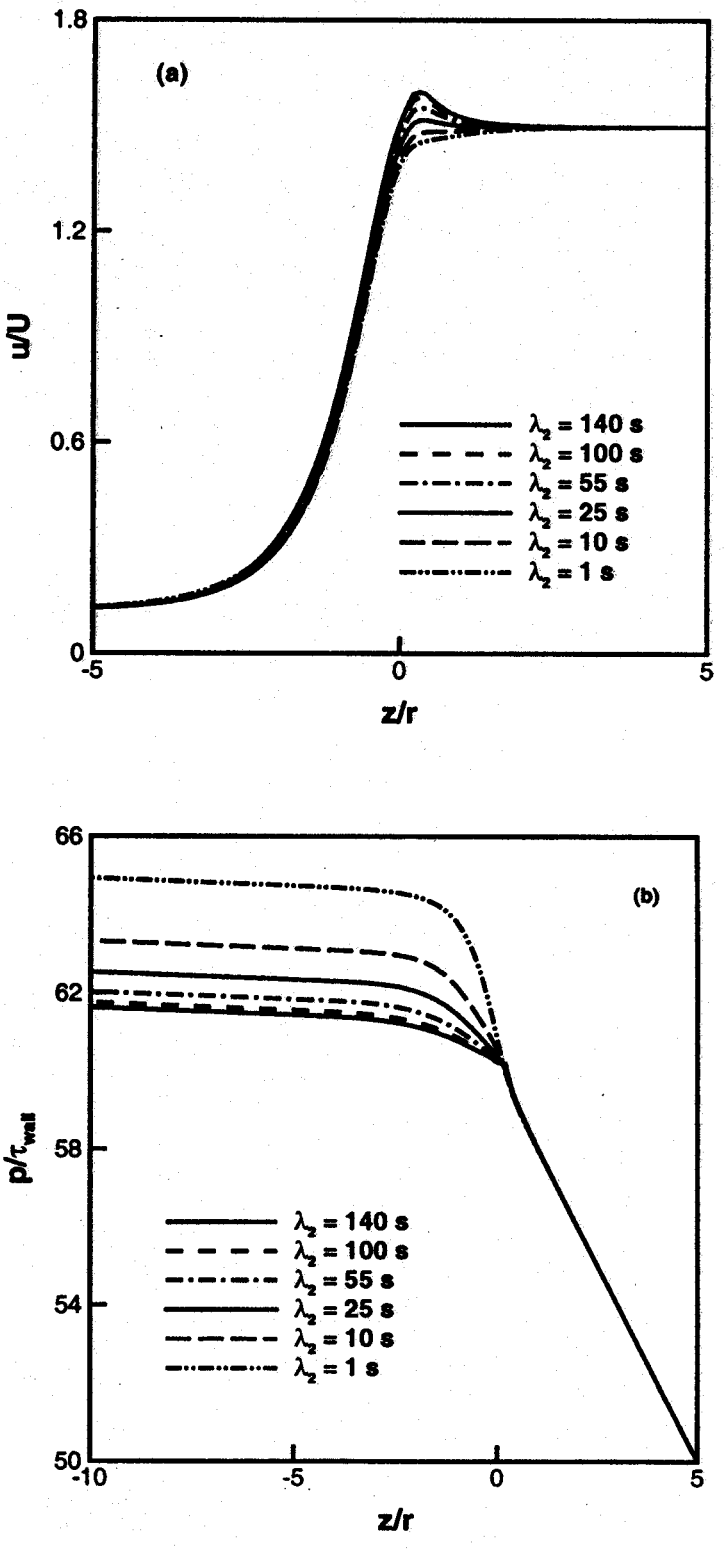

Figure 5. *Effect of λ_2 on the velocity (a) and pressure (b) along the center-line at $\dot{\gamma}_a = 1\ s^{-1}$ for $\lambda = 10$ s, n = 0.25, $\delta = 0$ and m = 0.5. It is noted that for $\delta = 0$, λ_1 has no effect on elongational viscosity.*

REFERENCES

1. Bird, R. B., Armstrong, R. C. and Hassager, O. *Dynamics of Polymeric Liquids*, Vol. 1, Wiley, (1987).
2. Carreau, P. J., Ph.D. Thesis, University of Wisconsin, Madison (1968).
3. Yasuda, K., Ph.D. Thesis, MIT, Cambridge (1979).
4. Cross, M. M., *J. Colloid Sci.*, **20**, 417 (1965).
5. Munstedt, H., *J. Rheol.*, **24**, 847 (1995).
6. Luan, H. M., in *Rheology*, Vol. 2: Fluids, G. Astarita, G. Marucci and L. Nicolais (eds.), Plenum, New York, 419–424 (1980).
7. Stevenson, J. F., *AICHE J.*, **18**, 540 (1972).
8. Meissner, J., *Chem. Engr. Commun.*, **33**, 159 (1985).
9. Larson, R. G., *Constitutive Equations for Polymeric Melts and Solutions*, Butterworths, Boston (1988).
10. Keunings, R., Chapter 9 in *Fundamentals of Computer Modelling for Polymer Processing*, C. L. Tucker (ed.), Hanser, Munich (1989).
11. Debbaut, B., Marchal, J. M. and Crochet, M. J., *J. Non-Newtonian Fluid Mech.*, **29**, 119 (1988).
12. Rajagopalan, D., Armstrong, R. C. and Brown, R. A., *J. Non-Newtonian Fluid Mech.*, **36**, 159 (1990).
13. Bolch, A., Townsend, P. and Webster, M. F., *J. Non-Newtonian Fluid Mech.*, **54**, 285 (1994).
14. Guenette, R. and Fortin, M., *J. Non-Newtonian Fluid Mech.*, **60**, 27 (1995).
15. Purnode, B. and Crochet, M. J., *J. Non-Newtonian Fluid Mech.*, **65**, 269 (1996).
16. Gupta, M. Hieber, C. A. and Wang, K. K. *Int. J. Numer. Meth. Fluids*, **24**, 493 (1997).
17. Beraudo, C., Fortin, A., Coupez, T., Demay, Y., Vergnes, B. and Aggasant, J. F., *J. Non-Newtonian Fluid Mech.*, **75**, 1 (1998).
18. Xue, S. C., Phan-Thein, N. and Tanner, R. I., *J. Non-Newtonian Fluid Mech.*, **74**, 197 (1998).
19. Moller, J. C., Lee, D., Kibbel, B. W. and Mangapora, L., *J. Non-Newtonian Fluid Mech.*, **35**, 1440 (1985).
20. Kwon, T. H., Shen, S. F. and Wang, K. K., *Polym. Eng. Sci.*, **26**, 214 (1986).
21. Oliveira, P. J. and Pinho, F. T., *J. Non-Newtonian Fluid Mech.*, **78**, 1, (1998).
22. Schunk, R. and Scriven, L. E., *J. Rheol.*, **34**, 1085 (1990).
23. Souza Mendes, P. R., Padmanabhan, M., Scriven, L. E. and Macosko, C. W., *Rheol. Acta.*, **34**, 209 (1995).
24. R. L. Thompson, P. R. Souza Mendes, M. F. Naccache, *J. Non-Newtonian Fluid Mech.*, **86**, 375 (1999).
25. Mitsoulis, E., Vlachopoulos, J. and Mirza, F. A., *Polym. Eng. Sci.*, **25**, 677 (1985).
26. Gupta, M., *SPE ANTEC Tech. Papers*, **45**, 1254 (1999).
27. Gupta, M., *SPE ANTEC Tech. Papers*, **45**, 83 (1999).
28. Gupta, M., *Polym. Eng. Sci.*, **40**, 23 (2000).
29. Gupta, M., "Simulation of Planar Entrance Flow Using Strain-Rate-Dependent Shear and Elongational Viscosities," *J. Reinforced Plastics and Composites*, (in press).
30. Quinzani, L. M., Armstrong, R. C. and Brown, R. A., *J. Non-Newtonian Fluid Mech.*, **52**, 1 (1994).